SOILS AND FOUNDATIONS Vol. 44, No. 5, 85-93, Oct. 2004
Japanese Geotechnical Society

ON THE LINEAR SEISMIC RESPONSE OF SOILS WITH MODULUS VARYING AS A POWER OF DEPTH—THE MALIAKOS MARINE CLAY

THALEIA TRAVASAROU[i] and GEORGE GAZETAS[ii]

ABSTRACT

The dynamic response of a soft and thick marine clay layer subjected to vertically propagating shear waves is obtained analytically. The deposit constitutes the topmost layer which will support a major 3.6 km long immersed tunnel in a high-seismicity region of central Greece. S-CPTU measurements show that the soil shear wave velocity varies with depth as $V_s = mz^{p/2}$, i.e. with a zero value at the surface. It is shown analytically that the shear strain just beneath the ground surface of such a deposit *either vanishes or tends to infinity*, depending on the exact rate of increase of the shear wave velocity with depth, as reflected in the parameter p. The steady-state response is also studied and an analytical expression for the amplification ratio is provided, while the consequences of soil nonlinearity are highlighted.

Key words: amplification, dynamic analysis, elastic analysis, inhomogeneous soil, seismic response, shear strain, shear wave velocity (**IGC**: C3/D7/E8)

INTRODUCTION

It is not rare in marine sediments that the shear modulus of the soil at the surface is nearly zero. Such a marine soil deposit was found under the seabed of a planned 3.6-km long immersed highway tunnel which will bridge Maliakos Gulf in central Greece. The seismic behavior of this structure depends on the dynamic displacements imposed by the surrounding soil. The dynamic response of the soil deposit was therefore of prime interest, and motivated the analyses and the subsequent research reported in this paper.

With design accelerations of 0.35 g at stiff ground outcrop, the first numerical results of the *equivalent linear* response of the soil exhibited *no* convergence, implying that acceleration and strains tend to become very large at the surface. To verify this result, an analytical study was initiated and is reported herein. A general, at first surprising, conclusion is drawn from the linear studies: the seismic strains in the soft soil at the ground surface tend to infinity under the assumption of linearity.

Based on the Maliakos Gulf case history, the scope of this paper is to analytically demonstrate the infinite growth of the dynamic elastic motion at the surface of a soil deposit, when the shear modulus varies according to a certain manner with depth, having zero value at the ground surface.

BRIEF REVIEW OF PREVIOUS RESEARCH

Several researchers have previously studied the dynamic characteristics of soils having continuously varying stiffness with depth. In his doctoral thesis Dobry (1971) investigated the free and forced vibration of soils where the increase of shear wave velocity with depth was represented by $V_s = c_0 z^{p/2}$. He developed closed-form expressions for the fundamental periods and mode shapes, and showed that under certain conditions the shear strain at the free surface does not necessarily tend to zero. Gazetas (1982), studied the effect of the rate (μ) and type (m) of heterogeneity on the fundamental period and the dynamic response of a soil deposit with shear wave velocity increasing from a non-zero value c_0 at the free surface to $V_s = c_0(1+\mu z)^m$, at depth z, with m taking the values 1, 2/3, 1/2, and 1/4. He came to the conclusion that the closer to uniform the distribution of velocity with depth is (i.e. the smaller m is), the larger the fundamental period of this layer becomes for the same average velocity. More importantly he revealed a very sharp increase of modal amplitudes near the surface with $m=1$ and $m=2/3$. This is indicative of a rapid growth of the shear strain close to the free surface.

Based on borehole data at the Shin-Ohta site in Japan, Towhata (1996) has convincingly generalized the above studies. He showed that the shear wave velocity can vary continuously with depth, even despite changes in the soil type (i.e., for soil ranging from reclaimed fill to alluvium). He then studied the dynamic response of a profile

[i] Post-Doctoral Researcher, University of California, Berkeley, USA.
[ii] Professor of Geotechnical Engineering, National Technical University, Athens, Greece (gazetas@ath.forthnet.gr).
Manuscript was received for review on January 14, 2003.
Written discussions on this paper should be submitted before May 1, 2005 to the Japanese Geotechnical Society, 4-38-2, Sengoku, Bunkyo-ku, Tokyo 112-0011, Japan. Upon request the closing date may be extended one month.

Table 1. Natural frequencies, natural periods and modal shapes of soils with varying shear modulus with depth

S-wave velocity or shear modulus	Reference	Fundamental periods/ frequencies ($n=1, 2 \ldots$)	Modal shapes
$V_s=c_0 z^{p/2}$	Dobry (1971)	$\omega_n=\frac{2-p}{2}\cdot\frac{c_0}{H^{(1/2)(1-p)}}\cdot q_n$ H: depth of deposit q_n: nth root of $J_j(q)$	$U_n(\tilde{z})=\frac{\Gamma(j+1)}{(q_n/2)^j}\tilde{z}^{(1/2)(1-p)}\cdot J_j(q_n\tilde{z}^{(1/2)(2-p)})$ $n=1, 2, \ldots$ modal number $\tilde{z}=z/H$ normalized depth $\Gamma(x)$: Gamma function of x q_n: nth root of $J_j(q)$ $J_j(x)$: Bessel function of order j with argument x
$V_s=c_0(1+\mu z)^{2/3}$	Gazetas (1982)	$T_n=\frac{4H}{c_0}\cdot\frac{3\pi}{2\tilde{\mu}S_n}$ H: depth of deposit $\tilde{\mu}=\mu H$ S_n: numerically recovered eigenvalues of the characteristic equation.	$U_n(\tilde{z})=(1+\tilde{\mu}\tilde{z})^{-1/3}\sin(S_n[(1+\tilde{\mu}\tilde{z})^{1/3}-(1+\tilde{\mu})^{1/3}])$ $\tilde{z}=z/H$ normalized depth $\tilde{\mu}=\mu H$ S_n: numerically recovered eigenvalues of the characteristic equation.
$G=A(z+z_0)^m$	Towhata (1996)	$T_1=\frac{4\pi}{(2-m)\xi_H}\cdot\sqrt{\frac{\rho}{A}}\cdot H^{(2-m)/2}$ ξ_H: argument that leads to the first zero of the displacement at the surface ρ: soil density A: shear modulus parameter	for $0<n<2$ $U_1(z)=\frac{C_3}{\rho\omega^2\sqrt{z+z_0}}\left[Y_\nu(\xi_0)\left\{J_\nu(\xi)-\frac{2-m}{2}\xi J_{\nu+1}(\xi)\right\}-J_\nu(\xi_0)\left\{Y_\nu(\xi)-\frac{2-m}{2}\xi Y_{\nu+1}(\xi)\right\}\right]$ C_3: constant parameter $\xi=\lambda(z+z_0)^{(2-m)/2}$ $\xi_0=\lambda z_0^{(2-m)/2}$ $\lambda=\frac{2}{2-m}\sqrt{\frac{\rho\omega^2}{A}}$ J_ν, Y_ν: Bessel functions of first and second kind respectively and order ν

where the shear modulus varies with depth according to $G=A(z+z_0)^n$. His formulation allowed for the modulus (or the shear wave velocity) to vanish at the free surface if $z_0=0$. Towhata showed that when this is the case, the displacement at the surface grows infinitely large. The main formulae of the above research efforts are summarized in Table 1.

MALIAKOS GULF IMMERSED TUNNEL AND SOIL CHARACTERIZATION

A 3.6 km-long immersed tunnel is currently being designed in a seismically sensitive region of Greece, bridging the gulf of Maliakos. The geotechnical exploration program, which included extensive in-situ and laboratory testing both offshore and onshore, has revealed the existence directly under the tunnel of a very soft normally consolidated clay (hereafter called *Soft "Maliakos" Clay*) of variable thickness, reaching about 30 m, and covering about 2/3 of the total bridging length. Both shear modulus and shear strength of this layer increase almost linearly with depth and approach zero at the free surface. Figure 1 gives a section of the soil profile along the tunnel line. Typical in-situ test data are shown in Fig. 2. Indicative of the low mechanical characteristics of the soft clay is the consistently near zero N values of the SPT test ($N_{SPT}=0$–2), the small values of the cone tip resistance q_c, the high values of porewater pressures u_{CPT} of the Cone Penetration CPTU tests, and the small values of the field vane shear strength. The latter however, with values of merely 10 kPa at a depth of 10 m, are far more erratic than the CPTU data. A plasticity index of PI = 30 and a density increasing with depth with a mean value of $\rho=1.6$ t/m^3 have also emerged from the laboratory tests.

Direct measurements of the shear wave velocity through Crosshole and Downhole tests were only performed in different positions onshore, while extensive seismic cone penetration testing CPTU was performed both offshore and onshore. It was concluded that the offshore layer referred to as *Soft "Maliakos" Clay* extends onshore for a distance of at least 1 to 2 km. The differences in the stiffness of the Soft Clay onshore and offshore, which can be observed in Fig. 2, reflect the additional consolidation due to the onshore alluvial cover. The elastic shear wave velocity $V_{S,0}$ (i.e. at very small strains, $\gamma<10^{-5}$) was then correlated with the value of the cone tip resistance q_c. The results, which are presented in Fig. 3, suggest that the correlation of the shear wave velocity and tip cone resistance (q_c) offshore is best described by:

$$V_{S,0}=150q_c^{1/2} \quad (1)$$

Due to the linear dependence of q_c on z,

$$V_{S,0}=30z^{1/2} \quad (2)$$

which implies continuous variation of the shear wave

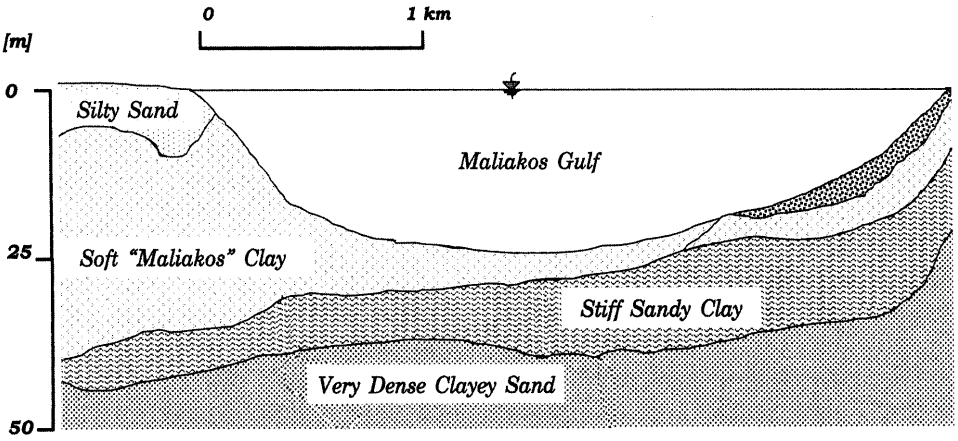

Fig. 1. Schematic cross-section of the soil profile along the tunnel line

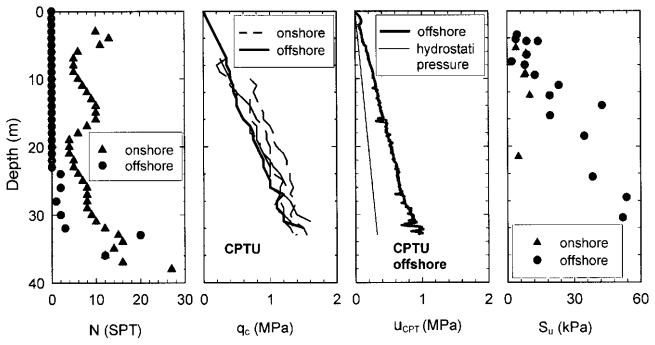

Fig. 2. Typical in-situ test data in the soft "Maliakos" Clay offshore and onshore as obtained from the standard penetration test, cone penetration test, and field vane test

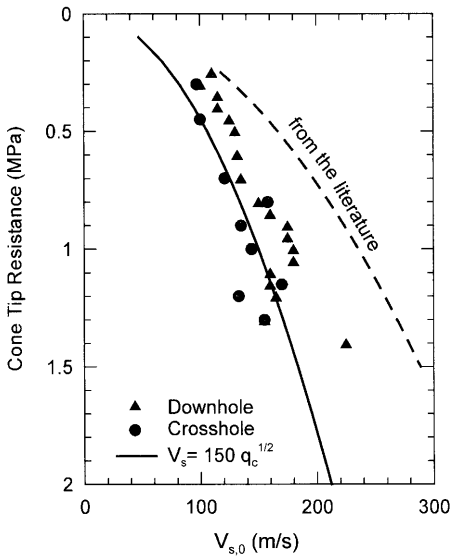

Fig. 3. Empirical correlation between small-strain shear wave velocity and tip resistance of the CPT test

velocity with depth. Admittedly, the data in Fig. 3 do not unequivocally support the assumption of zero stiffness at the surface of the soft clay may. However, this assumption is consistent with the dependence of the shear modulus on the effective overburden stress, which is zero at the soil surface. Furthermore, this assumption is supported by the truly zero values of both Standard and Cone Penetration tests. Note that zero value of the shear modulus at the soil surface has been used by many other researchers (e.g. Afra and Pecker, 2001) in their analytical derivations. (*See* also the classical work of Gibson, 1967, 1974.) Finally, the rationality of the assumed rate of increase of the shear wave velocity with depth can be confirmed by actual data of the soil stiffness (e.g. Lu et al., 1991; Fumal et al., 1981, etc.).

Additionally, the geotechnical exploration revealed the existence of a stiff clay layer underlying the soft "Maliakos" clay and extending to a depth of 60 to 80 meters. With a liquidity index of about 0.3 and a density of 2.1 t/m^3 the stiff clay has substantially better mechanical properties compared to the soft "Maliakos" clay. However, a detailed characterization of this stiff clay was left for the final design stage. For this stiff clay, the shear wave velocity profile was constructed based on the results of one crosshole test performed onshore and reaching a depth of 50 meters. Moreover, a linear variation of the shear wave velocity with depth was assumed based on the fact that the shear wave velocity is still affected by the vertical effective overburden stress at this depth. Synthesis of all available information led to the idealized soil profile depicted in Fig. 4, which was subsequently used in all dynamic response analyses.

EQUIVALENT LINEAR SEISMIC RESPONSE

At first the seismic response of the Soft Clay was evaluated using one-dimensional equivalent linear dynamic analysis (SHAKE type, i.e. Schnabel et al., 1972), which can only account for the possible nonlinear soil behavior iteratively, by adjusting the values of the shear modulus and damping ratio to the strain level induced by the shaking. The use of one-dimensional analysis is justified by the very smooth geometry of the problem. The variation of the shear wave velocity with depth used in the soil response analyses was already presented in Fig. 4, where the thickness of the soft clay

layer was parametrically varied to 20, 32, and 40 meters. The degradation of the shear modulus and hysteretic damping with increasing shear strain was modeled using the modulus reduction and damping curves proposed by Vucetic and Dobry (1991) for cohesive soils with PI = 30 and PI = 15 for the soft and stiff clay respectively.

Three input motions were selected for use in the dynamic response analyses, the main characteristics of which are summarized in Table 2. The selection was based on the agreement of the recorded peak values (i.e. peak ground acceleration and peak ground velocity) with the values corresponding to a return period of 500 years computed in a separate probabilistic seismic hazard analysis for the region (Gazetas, 1997). Still, the acceleration-time histories were selected to have different duration characteristics with the intent to explore the effect of duration on the dynamic response of the soft soil profile. Figure 5 presents the acceleration response spectra for 5% damping of the three excitations.

The response of the soil column was initially computed, after scaling all three motions to a peak acceleration of 0.35 g at the bedrock. *Convergence, however, failed to occur!* Then, a lower value of peak acceleration was applied as excitation. Convergence was finally accomplished only after setting the maximum acceleration at a mere 0.05 g. Still, despite this small amplitude of the excitation both the maximum shear strain and the peak ground acceleration were enormously magnified, at the surface. This magnification was in fact, a sensitive function of the thickness of the layers into which the top of the soil was discretized. For a thickness of the top layer of 0.20 m:

$$a_{max} \approx 0.35\ \text{g}, \quad \text{and} \quad \gamma_{max} \approx 10\%. \tag{3}$$

Even larger values were computed with a topmost layer thickness of 0.10 m, and so on.

Figure 6 depicts the variation of the peak acceleration and the peak shear strain in the uppermost 5 meters of the idealized soil profile computed for the 32-meter deep

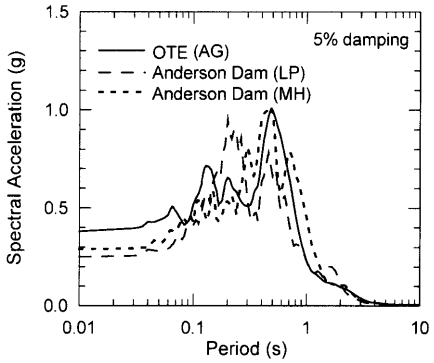

Fig. 5. Acceleration response spectra for 5% damping of the recordings used as input motions in the dynamic site response analyses

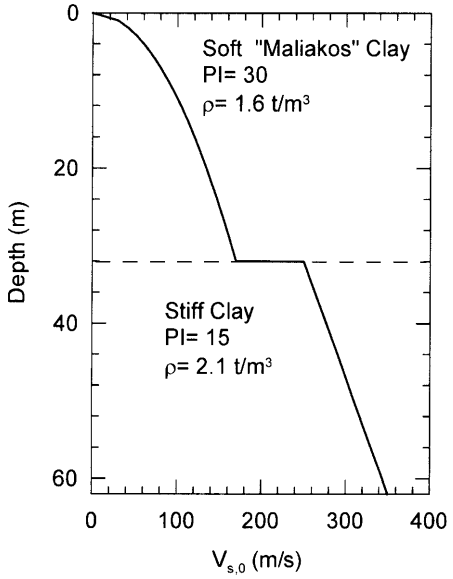

Fig. 4. Variation of small-strain shear wave velocity with depth in the idealized soil profile used in the dynamic response analyses

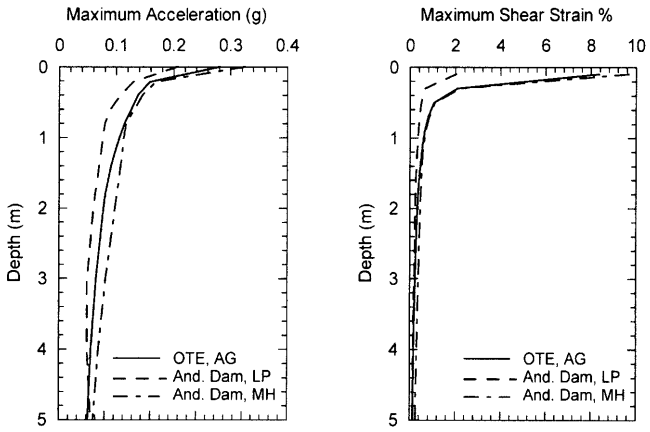

Fig. 6. Typical amplification of the maximum horizontal acceleration and the maximum shear strain close to the surface of the inhomogeneous profile as computed by the equivalent linear analyses

Table 2. Ground motion characteristics of the three records used as input in the dynamic response analyses

Record	Earthquake[1)]	M	R[2)] (km)	PGA (g)	PGV (cm/s)	PGD (cm)	T_m (s)	T_p (s)	D_{5_95} (s)	Forward directivity
OTE[3)]	AG (1995)	6.2	5.0	0.38	40	4	0.55	0.48	4	yes
Anderson Dam	LP (1989)	6.9	21.4	0.25	22	7	0.47	0.20	18	no
Anderson Dam	MH (1985)	6.2	2.6	0.29	28	6	0.55	0.48	10	no

[1)] AG: Aegion, Greece, LP: Loma Prieta, USA, MH: Morgan Hill, USA.
[2)] Rupture distance
[3)] This record is a deconvolved record obtained from a 1-D equivalent linear analysis with the original recording used as input at the surface.

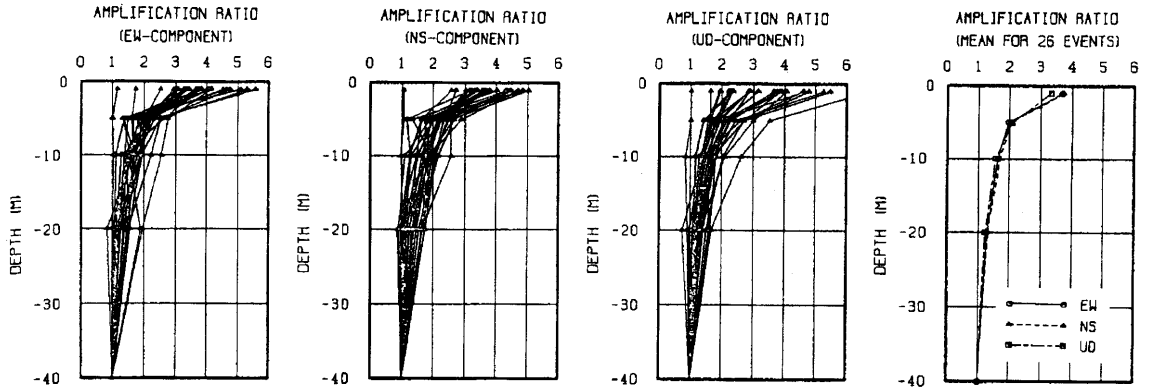

Fig. 7. Amplification ratios of peak ground acceleration recorded in borehole C_0 of the Chiba array in Japan (from Lu et al., 1991)

layer of soft "Maliakos" clay and for the three input motions with peak acceleration at the base equal to 0.05 g. This behavior was found to be insensitive to variations in either the characteristics of the excitation or the total thickness of the soft clay layer. In addition, as already mentioned, the final results are strongly dependent on the discretization of the soil deposit into homogeneous layers of progressively increasing stiffness: the thinner these layers are just below the surface, the greater is the magnitude of the computed peak ground motion (acceleration and strain). Note that with a very fine discretization of the soil profile, the inhomogeneity in shear modulus is approximated with greater accuracy (and it precisely alludes to the actual concept of $V_s \to 0$ as $z \to 0$).

This behavior prompted the analytical study described in the sequel. When a soil deposit undergoes large deformation it degrades in stiffness. It is customary to describe such behavior in terms of an equivalent-linear stiffness, compatible with the amplitude of the shear strain. In the case of the Maliakos soft clay layer, the strain-compatible shear wave velocity profile obtained at the final iteration of the equivalent linear analysis, was approximated with the following analytical expression:

$$V_s \approx 16 z^{2/3} \tag{4}$$

This expression was found to be valid in all cases, independently of the specific characteristics of the excitation and the exact depth of the soft clay layer. Notice that the variation of velocity in Eq. (4) exhibits a more rapid increase with depth (2/3 power) than Eq. (2) (1/2 power)—this is understandable in view of the larger shear strains (and hence the increased softening) as one approaches the ground surface.

The rapid growth of the maximum horizontal acceleration within only a few meters from the soil surface in relatively soft clayey deposits with continuous variation of the shear wave velocity with depth has been captured, although infrequently, by downhole arrays. Figure 7 offers convincing evidence of such a case, reported by Lu et al. (1991). The authors explored the amplification characteristics of a 40-meter deep soil deposit composed of mainly clay having small values of the standard penetration resistance at shallow depths (i.e. $N \sim 5$ at 0–5 meters) and shear wave velocity increasing with depth at a rate very similar to that of Eq. (4). Using the downhole recordings from 26 earthquake events, with magnitudes ranging between 4.0 and 7.9, at epicentral distances from 5 km to 702 km, the authors concluded that: "... *the amplification of peak acceleration mostly occurred at a few meters below the ground surface, which is considered to be caused by the top soft layer.*" (Lu et al., 1991).

RIGOROUS ELASTIC ANALYSIS

It was concluded from the numerical analyses that exceedingly large amplification at the surface of the soft clay tends to develop when the shear wave velocity profile is described by expressions (2) and (4). The persistence of these results motivated the search for an analytical verification. Such an analytical solution, aimed at explaining and generalizing the phenomenon, is thus presented here. The problem to be solved is defined as follows:

A soil deposit of thickness H, constant density ρ, and shear wave velocity varying with depth as

$$V_s = m z^{2/3}, \tag{5}$$

is excited by vertically propagating horizontal shear waves described by the harmonic base displacement

$$u = U e^{i\omega t}. \tag{6}$$

The deposit overlies rigid rock. Equilibrium of an arbitrary soil element in the horizontal direction yields

$$\frac{\partial \tau}{\partial z} = \rho \frac{\partial^2 u(z,t)}{\partial t^2} \tag{7}$$

which upon substituting:

$$\tau = G(z)\frac{\partial u}{\partial z}, \quad G = \rho V_s^2 \quad \text{and} \quad \Re_o = \frac{\omega}{m} \tag{8}$$

yields the governing equation of motion:

$$\boxed{z^2 U''(z) + \frac{4}{3} z U'(z) + \Re_o^2 z^{2/3} U(z) = 0} \tag{9}$$

The above differential equation is a Bessel Differential

Equation, the solution of which is given by

$$U(z)=z^{-1/6}[c_1 J_{1/2}(3\Re_o z^{1/3})+c_2 Y_{1/2}(3\Re_o z^{1/3})] \quad (10)$$

where J and Y are the Bessel functions of first and second kind, respectively, and order 1/2 (i.e. Abramowitz and Stegun, 1970). Since

$$\left.\begin{aligned} J_{1/2}(x)&=\sqrt{\frac{2}{\pi x}}\sin x \\ Y_{1/2}(x)&=-\sqrt{\frac{2}{\pi x}}\sin x \end{aligned}\right\} \quad (11)$$

where

$$x=3\Re_o z^{1/3}, \quad (12)$$

and defining

$$c_{11}=\sqrt{\frac{2}{3\pi}}\cdot c_1, \quad c_{22}=\sqrt{\frac{2}{3\pi}}\cdot c_2 \quad (13)$$

the amplitude of the displacement and its derivative with respect to z (representing shear strain) are

$$U(z)=\frac{1}{\sqrt{\Re_o}}z^{-1/3}[c_{11}\sin(3\Re_o z^{1/3})+c_{22}\cos(3\Re_o z^{1/3})] \quad (14)$$

$$U'(z)=\frac{1}{\sqrt{\Re_o}}z^{-1/3}\left[\left(-\frac{c_{11}}{3}z^{-1}-c_{22}\Re_o z^{-2/3}\right)\sin(3\Re_o z^{1/3})+\left(c_{11}\Re_o z^{-2/3}-\frac{c_{22}z^{-1}}{3}\right)\cos(3\Re_o z^{1/3})\right] \quad (15)$$

Natural Frequencies of the Soil Deposit

In the absence of external excitation, the eigenvalues of the system are derived by enforcing the two boundary conditions:

- Shear stresses vanish at the surface of the soil

$$\lim_{z\to 0}\tau_{zx}=\lim_{z\to 0}\left(G\frac{\partial u}{\partial z}\right)=\lim_{z\to 0}\left(z^{4/3}\frac{\partial u}{\partial z}\right)=0 \quad (16)$$

- Displacements vanish at the interface between the soft soil and the baserock

$$U(z=H)=0 \quad (17)$$

From the first boundary condition and with $c_{11}=c$:

$$U(z)=\frac{c}{\sqrt{\Re_o}}z^{-1/3}\sin(3\Re_o z^{1/3}) \quad (18)$$

and, then, the second leads to

$$3\Re_o H^{1/3}=n\pi \quad (19)$$

from which the natural frequencies are uncovered

$$\boxed{\omega_n=\frac{n\pi}{3}\frac{m}{H^{1/3}}} \quad n=1, 2, \ldots \quad (20)$$

The natural periods are therefore

$$T_n=\frac{6}{n}\frac{H^{1/3}}{m} \quad (21)$$

For comparison, the natural periods of the corresponding homogeneous soil deposit having thickness H and constant shear wave velocity $\bar{V}_s$ computed by Eq. (22) are given by Eq. (23):

$$\bar{V}_s=\frac{\int_0^H V_s\,dz}{\int_0^H dz}=\frac{3}{5}mH^{2/3} \quad (22)$$

$$T_n=\frac{1}{2n-1}\frac{4H}{\bar{V}_s}=\frac{20/3}{2n-1}\cdot\frac{H^{1/3}}{m} \quad (23)$$

For $n=1$ the two equations (21 and 23) give, respectively

$$(T_1)_{\text{in hom}}=6\frac{H^{1/3}}{m} \quad \text{and} \quad (T_1)_{\text{hom}}=6.67\frac{H^{1/3}}{m} \quad (24)$$

while $T_2/T_1=1/2$ for the inhomogeneous deposit, compared with $T_2/T_1=1/3$ for the equivalent homogeneous.

To get the eigenmodes of the soil deposit it suffices to substitute (20) into (18)

$$\boxed{U_n(z)\propto\frac{1}{H^{-1/6}}z^{-1/3}\sin\left(n\pi\left(\frac{z}{H}\right)^{1/3}\right)} \quad (25)$$

Infinite Shear Strain at the Soil Surface

The shear strain at the surface of the soil deposit is given by Eq. (15), with $c_{22}=0$ (which stems from the first boundary condition) and $c_{11}=c$:

$$U'(z)=\frac{1}{\sqrt{\Re_o}}z^{-1/3}\left[-\frac{c}{3}z^{-1}\sin(3\Re_o z^{1/3})+c\Re_o z^{-2/3}\cos(3\Re_o z^{1/3})\right] \quad (26)$$

It can be verified after some straightforward algebra that the limit, as $z\to 0$ is

$$\frac{c}{\sqrt{\Re_o}}\lim_{z\to 0}\left[\frac{1}{z}\left(\Re_o\cos(3\Re_o z^{1/3})-\frac{\Re_o}{3}\frac{\sin(3\Re_o z^{1/3})}{\Re_o z^{1/3}}\right)\right]\to\infty \quad (27)$$

(simply recalling that as $x\to 0$, $\cos x\to 1$, and $(\sin x/x)\to 1$). In other words, the shear strain at the surface tends to infinity.

This interesting observation can be generalized: *the shear strain at the surface would either tend to zero (0) or tend to infinity (∞), depending only on the rate of increase of the shear wave velocity with depth.*

Indeed, for the most general case of shear wave velocity increasing according to:

$$V_S=mz^{p/2} \quad (28)$$

Dobry et al. (1971) had shown that the normalized eigenmodes are given by

$$\tilde{U}_n(Z)=\frac{\Gamma(j+1)}{(q_n/2)^j}Z^{(1/2)(1-p)}J_j(q_n Z^{(1/2)(2-p)}], \quad n=1, 2, \ldots \quad (29)$$

where: $\Gamma(x)$ = Gamma function of x
J_j = Bessel function of order j
$q_n = n^{\text{th}}$ root of $J_j(q)$

$Z=z/H$, normalized depth

Using their results we can easily show that shear strains at the surface *tend to zero when* $0<p<1$, but that when $p>1$, which is indeed the case for the Soft Clay of Maliakos (where $p=4/3$),

$$\gamma(0)\propto \tilde{U}_n'(0)\to\infty \tag{30}$$

i.e., the shear strain at the surface *tends to infinity*. On the other hand, when the shear modulus at the surface has any non-zero value, the boundary condition of zero shear stress imposes invariably the condition of $\gamma(0)=0$.

Natural Mode Shapes of the Soil Deposit

The maximum displacement at the surface is evaluated by the limit of Eq. (18) for $z\to 0$. Defining for each fundamental frequency:

$$\Re_{on}=\frac{\omega_n}{m}$$

we obtain

$$U_n(z=0)=\lim_{z\to 0}\left[\frac{c}{\sqrt{\Re_{on}}}z^{-1/3}\sin(3\Re_{on}z^{1/3})\right]$$
$$=3c\Re_{on}^{1/2}\lim_{z\to 0}\left[\frac{\sin(3\Re_{on}z^{1/3})}{3\Re_{on}z^{1/3}}\right]=3c\Re_{on}^{1/2} \tag{31}$$

The normalized modal shapes are therefore given by

$$\tilde{U}_n=\frac{U_n(z)}{U_n(0)}=\frac{\sin(3\Re_{on}z^{1/3})}{3\Re_{on}z^{1/3}}$$

from which

$$\boxed{\tilde{U}_n=\frac{1}{n\pi}\left(\frac{z}{H}\right)^{-1/3}\sin\left(n\pi\left(\frac{z}{H}\right)^{1/3}\right)} \tag{32}$$

As a reminder, the corresponding modal shapes of the homogeneous soil profile with the same thickness are given by:

$$\tilde{U}_n=\frac{U_n(z)}{U_n(0)}=\cos\left[(2n-1)\frac{\pi}{2}\frac{z}{H}\right] \tag{33}$$

The first five modes of the studied (inhomogeneous) soil profile, given by Eq. (32), are drawn in Fig. 8. Furthermore, Fig. 9 compares the first four mode shapes of the inhomogeneous soil profile and those of the corresponding homogeneous. We note that in the case of the inhomogeneous profile, there is a sharper attenuation of modal amplitudes with depth. The soil layer remains almost "inactive" below a depth of merely $z/H\approx 0.10$. The asymptotic way of the modal displacements as we approach the surface in the inhomogeneous stratum, is in clear agreement with the infinite growth of the peak shear strain at that level. On the contrary, the mode shapes of the homogeneous soil profile reach the surface being tangent to the vertical, implying a zero value of the shear strain.

Steady State Harmonic Response

The steady state response to a harmonic base excitation, $u(z,t)=U_h e^{i\omega t}$ is given by

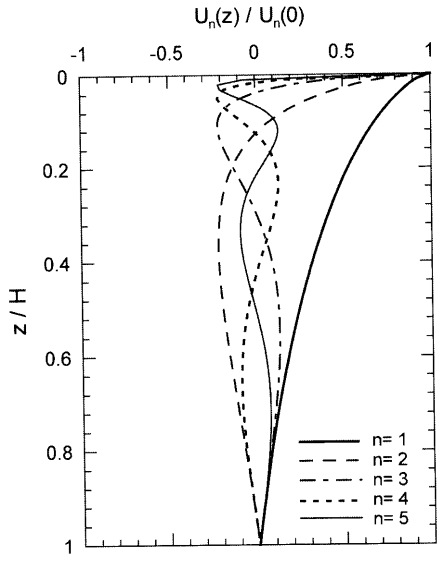

Fig. 8. Five first eigenmodes of the inhomogeneous soil with $V_s=mz^{2/3}$ computed using Eq. (32)

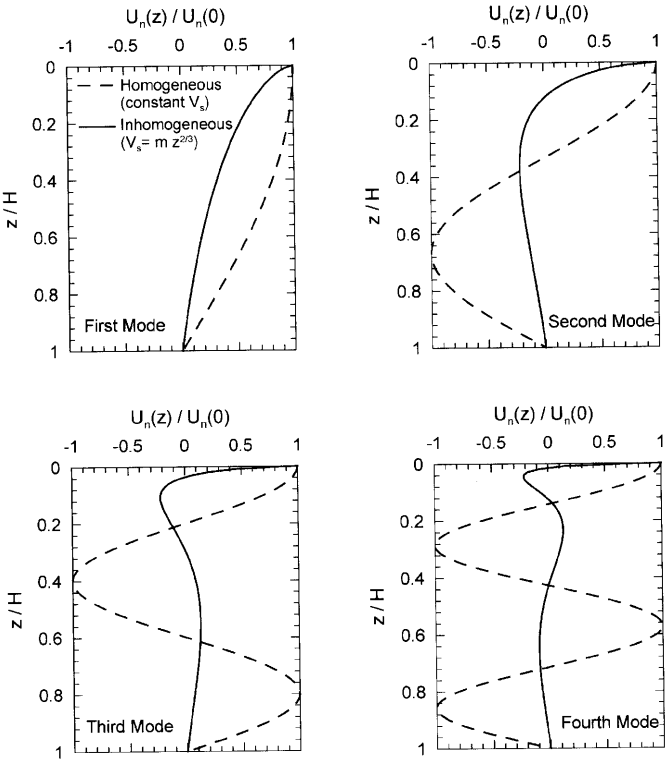

Fig. 9. Comparison of the first four eigenmodes of the inhomogeneous ($V_s=mz^{2/3}$) soil with those of a homogeneous deposit with the same depth

$$U(z)=U_h\left(\frac{H}{z}\right)^{1/3}\frac{\sin(3\Re_o z^{1/3})}{\sin(3\Re_o H^{1/3})} \tag{34}$$

Of particular interest is the amplitude of the amplification function, that is of the transfer function for the displacement at the surface from the displacement at the baserock. Since

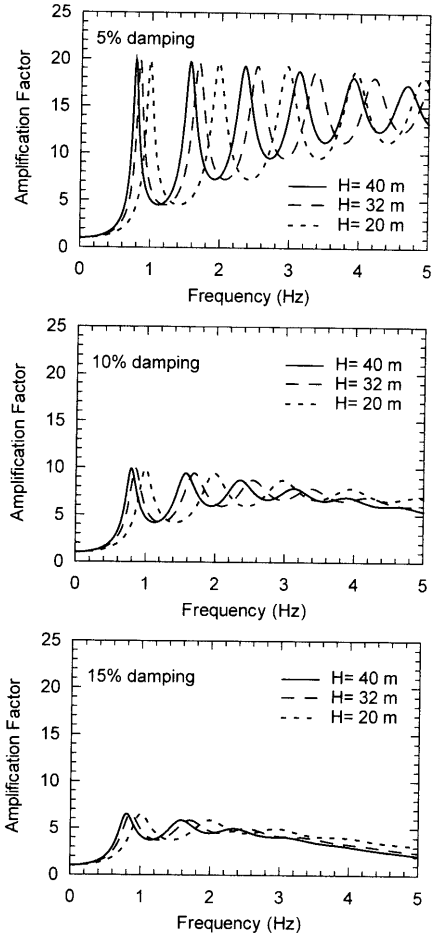

Fig. 10. Dynamic amplification factor computed by the analytical closed-form solution (i.e. Eq. (36)) for three different thickness values of the soft clay and three values of the damping ratio

$$U(0)=\lim_{z\to 0} U(z)$$
$$=U_h\frac{3\Re_o H^{1/3}}{\sin(3\Re_o H^{1/3})}\lim_{z\to 0}\left(\frac{\sin(3\Re_o z^{1/3})}{3\Re_o z^{1/3}}\right)$$
$$=U_h\frac{3\Re_o H^{1/3}}{\sin(3\Re_o H^{1/3})} \qquad (35)$$

the amplification factor becomes:

$$A=\frac{U(z=0)}{U(z=H)}=\frac{3\dfrac{\omega H^{1/3}}{m}}{\sin\left(\dfrac{3\omega H^{1/3}}{m}\right)} \qquad (36)$$

Soil damping can be accounted for in Eq. (36) by replacing m with a complex number equal to $m^*=m(1+i\xi)$. Figure 10 plots Eq. (36), for three values of the thickness of the soft Maliakos clay (i.e. $H=20$, 32, and 40 m) and three values of the damping ratio. Notice that the peak amplitudes attain a nearly constant value for all modes; only at very large damping ratios one sees a slightly decreasing importance of higher mode resonance —another cause of the infinite growth of elastic strains, displacements, and accelerations at the surface. By contrast, recall that for a homogeneous soil layer the peaks of the amplification function, A, are given by (e.g. Kramer, 1996):

$$A\approx\frac{2}{\pi}\frac{1}{\lambda(2n-1)},\quad n=1,2,\ldots, \qquad (37)$$

where λ = the hysteretic damping ratio. Evidently in the homogeneous soil layer the role of the higher natural modes becomes progressively smaller, and is usually negligible beyond the second mode.

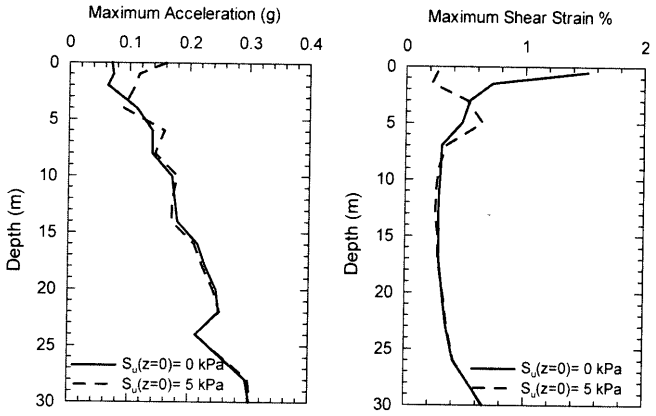

Fig. 11. Typical variation of the maximum horizontal acceleration and the maximum shear strain with depth for the inhomogeneous profile computed with nonlinear analyses. Two different assumptions are made for the value of the undrained shear strength at the ground surface

NONLINEAR RESPONSE

In addition to the theoretical value of the above conclusions, their practical usefulness is in interpreting the results of microtremors, which might lead to the high near surface amplifications as predicted by the linear theory. On the other hand, a strong seismic motion would lead to nonlinear response especially near the ground surface. Intense nonlinearity would reduce the transmitted accelerations to low values, mainly in function of the precise value of the actual soil strength $S_u(z\approx 0)$.

With this in mind nonlinear analyses were performed using the computer algorithm DESRA (Lee and Finn, 1978) in which the soil is modeled through a hyperbolic $\tau-\gamma$ monotonic relationship along with the Masing criterion for cyclic unloading and reloading. Identical soil profiles, in terms of soil stiffness, were used in the equivalent linear and nonlinear analyses. Additionally, the results of vane shear data performed in the soft "Maliakos" clay to a depth of 30 meters justified the use of an undrained shear strength, S_u, increasing with depth as $S_u=1.2z$. At the surface, the value of the undrained shear strength was parametrically varied to be zero and 5 kPa. The results were strongly dependent on the value of the shear strength at the ground surface. The vanishing of the shear strength serves as a cut-off, impeding the propagation of the shear waves and leading to a surface peak acceleration reduced to the very small value of 0.07 g as shown in Fig. 11. Notice however, that the

Masing criterion may substantially overpredict the soil damping, and therefore the results may underpredict reality.

CONCLUSIONS

An analytical closed-form solution was developed for the free and forced vibration of a linear elastic inhomogeneous soil deposit subjected to vertically propagating shear waves. The soil inhomogeneity is described by the variation of the shear wave velocity with depth according to $V_s = mz^{2/3}$. Such a variation can be typical of soft clay subjected to relatively weak ground motion. It was shown that for a linear elastic material the shear *strain* computed at the surface of the soft clay tends to infinity, despite the boundary condition of vanishing shear stress. This analytical finding is indirectly supported by downhole recordings in a soft-clay soil profile. Such recordings show that ground motion can be amplified significantly in the upper few meters of soft soil. Apparently, the trend of this amplification is controlled by the nearly zero value of the soil stiffness at the ground surface and the specific (relatively rapid) rate of increase of the shear wave velocity with depth.

ACKNOWLEDGMENTS

The authors wish to thank the Mr. Marios Apostolou for kindly providing Fig. 1.

REFERENCES

1) Abramowitz, M. and Stegun, I. (1970): *Handbook of Mathematical Functions*, Dover Publications.
2) Afra, H. and Pecker, A. (2001): Calculation of free field response spectrum of a non-homogeneous soil deposit from bed rock response spectrum, *Soil Dynamics and Earthquake Engineering*, **22**, 157–165.
3) Dobry, R., Whitman, R. V. and Roesset, J. M. (1971): Soil properties and the one-dimensional theory of earthquake amplification, Massachusetts Institute of Technology, Department of Civil Engineering, Research Report, R71–18.
4) Fumal, T. E., Gibbs, J. F. and Roth, E. F. (1981): Insitu measurements of seismic velocity at 19 locations in the Los Angeles California Region, Open-File Report 81–399, U.S. Geological Survey, 121.
5) Gazetas, G. (1982): Vibrational characteristics of soil deposits with variable wave velocity, *International Journal for Numerical and Analytical Methods in Geomechanics*, **6**, 1–20.
6) Gazetas, G. (1995): The Aegion (Greece) 15-6-1995 Earthquake: Analysis of damaged soft-first-story buildings with emphasis on the collapse of the administration building of E.B.O., *Bulletin of the Technical Chamber of Greece*, Athens, Issue 1883, 30–92.
7) Gazetas, G. (1997): Maliakos Tunnel: Synthesis of seismological, geophysical and geotechnical studies, Report to Public Works Department, Athens, Greece, **I and II**.
8) Gibson, R. E. (1967): Some results concerning displacements and stresses in a non-homogeneous elastic half-space, *Geotechnique*, **17** (1), 58–67.
9) Gibson, R. E. (1974): The analytical method in soil mechanics, *Geotechnique*, **24** (2), 115–140.
10) Kramer, S. L. (1996): Geotechnical Earthquake Engineering, Prentice Hall.
11) Lee, M. K. D. and Finn, W. D. L. (1978): Desra-2: Dynamic effective stress response analysis of soil deposits with energy transmitting boundary including assessment of liquefaction potential, Research Report, University of British Columbia.
12) Lu, L., Katayama, T. and Yamazaki, F. (1991): Soil amplification based on array observation in Chiba, Japan, *Proc. Second International Conference on Recent Advances in Geotechnical Earthquake Engineering and Soil Dynamics*, St. Louis, Missouri, Paper 8.9, 1181–1188.
13) Schnabel, P. B., Lysmer, J. and Seed, H. B. (1972): Shake: A computer program for earthquake response analysis of horizontally layered sites, Report EERC 72–12, University of California, Berkeley.
14) Towhata, I. (1996): Seismic wave propagation in elastic soil with continuous variation of shear modulus in the vertical direction, *Soils and Foundations*, **36** (1), 61–72.
15) Vucetic, M. and Dobry, R. (1991): Effect of soil plasticity on cyclic response, *Journal of Geotechnical Engineering*, **17** (1), 89–107.